Carrier distribution in (0001)InGaN/GaN multiple quantum well light-emitting diodes

Aurélien David,[a] Michael J. Grundmann, John F. Kaeding, Nathan F. Gardner, Theodoros G. Mihopoulos, and Michael R. Krames
Philips Lumileds Lighting Company, 370 W. Trimble Rd., San Jose, California 95131, USA

(Received 5 November 2007; accepted 20 December 2007; published online 4 February 2008)

We study the carrier distribution in multi quantum well (multi-QW) InGaN light-emitting diodes. Conventional wisdom would assume that a large number of QWs lead to a smaller carrier density per QW, enabling efficient carrier recombination at high currents. We use angle-resolved far-field measurements to determine the location of spontaneous emission in a series of multi-QW samples. They reveal that, no matter how many QWs are grown, only the QW nearest the *p* layer emits light under electrical pumping, which can limit the performances of high-power devices. © *2008 American Institute of Physics*. [DOI: 10.1063/1.2839305]

High-power GaN-based light-emitting diodes[1] (LEDs) require high injection currents which translate into high current densities J, on the order of $J_{high} \sim 100-1000$ A cm^{-2}. It is well known that the internal quantum efficiency η_{int} of InGaN/GaN quantum-well (QW) structures peaks at lower current densities $J_{max} \sim 1-10$ A cm^{-2}, and is lower by a factor of 2 at high J.[1–3] It was recently suggested that Auger recombination is the cause of this behavior.[4]

To maintain a high η_{int} at high J, a straightforward approach is to increase the number of QWs, thus spreading carriers and lowering their density in each QW for a given J. If the QWs are uniformly injected, the peak current J_{max} should scale as the number of QWs. In this letter, we show that only the QW closest to the *p*-GaN emits light in a typical (0001)-InGaN/GaN LED.

The data presented below were taken on three samples with two, four, and six QWs, respectively, emitting at $\lambda = 445$ nm. Their structure is similar to the QW samples described in Ref. 3, with QW and barrier thicknesses of 3 and 11 nm. The thickness of the *p* layers above the QWs is kept constant to $d = 116$ nm to ensure comparable injection properties. Thickness values were checked by x ray. We label QWs starting from the *p* side: the two QW sample only contains QWs 1 and 2, while the six QW sample contains QWs 1–6.

To estimate the quality of the QWs, we perform photoluminescence (PL) with excitation by a 375 nm InGaN laser. The laser is only absorbed by the QWs (~1% absorption per QW) so that the PL signal should be proportional to the number of QWs (although cavity effects in the GaN layer can slightly alter the laser absorption by each QW). Indeed, the PL signals for the two, four, and six QW samples are 1.0, 1.7, and 2.8, respectively (in arbitrary units), suggesting that the η_{int} of the QWs is uniform.

We then test the electroluminescence in a simple geometry, using a Ni layer as the *p* electrode under which luminescence occurs. Figure 1 displays the external efficiency (i.e., the radiometric light output divided by the current) of the samples versus J. All curves are nearly identical, as already reported on similar structures in Ref. 3. Notably, J_{max} is nearly constant, suggesting that the same number of QWs are injected in each sample even though the total number of QWs is varied.

In order to determine optically which QWs emit light, we use angle- and wavelength-resolved far-field pattern (FFP) measurements. Instead of Ni as a *p* contact, we now use Ag, which possesses strong reflectivity and enhances cavity effects. We measure the FFP emitted downward through the sapphire substrate, with a fiber mounted on a rotating arm located 10 cm away from the source. Spectra are collected at polar angles $\theta = 0°$ (vertical) to $\theta = 70°$, at a current density $J \sim 80$ A cm^{-2}, beyond the efficiency peak and well within the high-current regime which we seek to characterize.

Let us discuss the principle of the experiment. Each QW is located at a specific distance from the Ag mirror, which modulates its extraction efficiency by cavity effects.[5,6] Figures 2(a) and 2(b) show the epitaxial structure and theoretical extraction to air (integrated over the full half space) of each QW as a function of wavelength, computed by a scattering matrix method.[7] Figures 2(c) and 2(d) detail the corresponding calculated angle-resolved FFPs for QWs 1 and 6. Notice the Fabry–Pérot fringes due to the GaN cavity which modulates the FFP. Since intensity vanishes at large θ (because of Fresnel coefficients and solid angle effects), we normalize these plots in the θ direction by a function $\cos^2\theta$, which reveals the large-angle behavior. As can be seen, cavity ef-

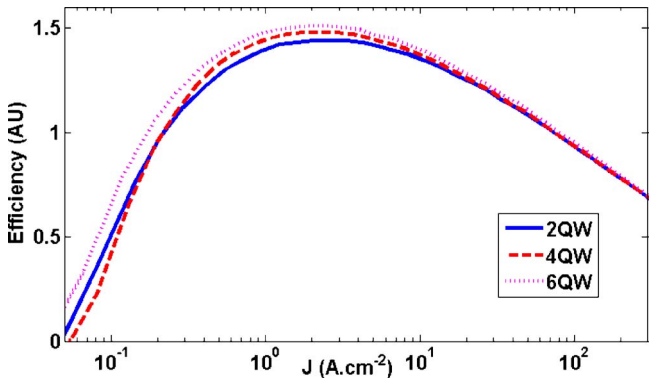

FIG. 1. (Color online) Efficiency vs. injection current for samples with two, four, and six QWs. The peak current J_{max} is identical for all structures, suggesting that the same number of QWs emit in all three structures. The peak emission wavelength at J_{max} is 445 ± 1 nm for all samples.

[a]Electronic mail: aurelien.david@philips.com.

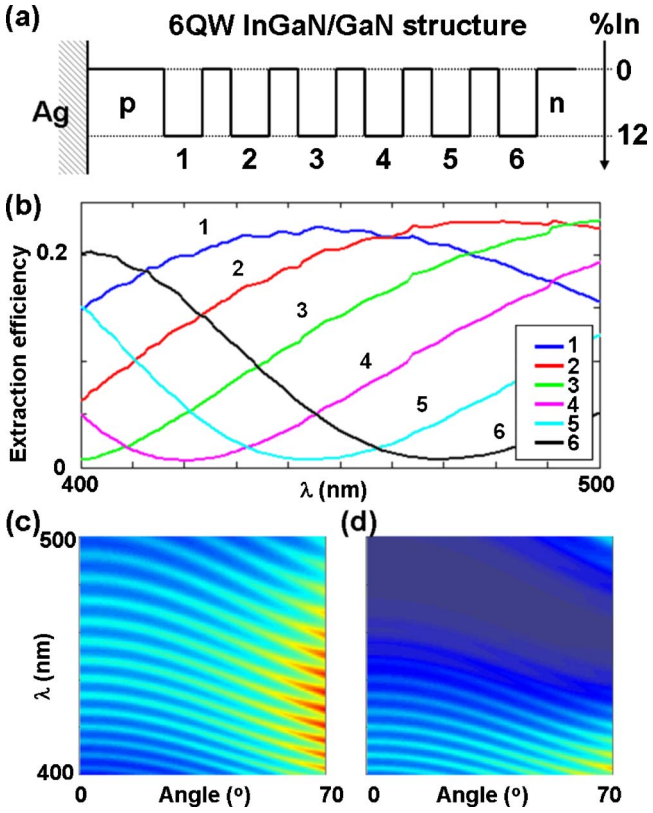

FIG. 2. (Color online) (a) Structure of the six-QW sample with corresponding QW numbers. (b) Calculated extraction efficiency of each QW. [(c) and (d)] Calculated far-field patterns of QWs 1 and 6, normalized by $\cos^2\theta$ to reveal the large angle behavior.

fects yield very different FFPs for different QWs. Since the *p*-layer thickness is constant, the distance d between a given QW and the Ag mirror is the same in all samples. The interference caused by the mirror yields maximum extraction at an angle θ and a wavelength λ satisfying the condition $4n\pi d\cos\theta_{in}/\lambda+\psi=2\pi m$, where n is the index of GaN, θ_{in} the inner angle corresponding to θ, ψ the phase shift of the mirror, and m an integer ($m=1$ here). Thus, each QW is efficient at extracting a specific range of wavelengths in a specific direction. In principle, the emitting QWs can thus be determined by fitting measured FFPs.

Figure 3(a) shows the experimental FFP for the two-QW sample. Unfortunately, the comparison with calculations is hindered by the spectral line shape of the QWs. Indeed, Figs. 2(b) and 2(c) correspond to a "white" source emitting a constant intensity at all wavelengths. The *exact* QW line shape is not known (and may vary from sample to sample and with J) and would be necessary to compare the measurements to the calculated FFPs. Rather, we resort to the following normalization procedure. An approximate line shape is estimated by integrating the experimental FFP over θ. After normalization by this line shape, the FFP is considerably "flatter," similar to those shown in Ref. 8. We then normalize the FFP a second time along λ (with a hand-defined smooth function) so that all the maxima of the Fabry–Pérot peaks of the FFP at $\theta=0°$ are pinned to 1. (Formally, the FFP can be expressed as $\mathrm{FFP}\sim Ay(L,\theta)\zeta(L,d,\theta)l(\lambda)-$ with Ay the Airy function representing the response of a passive Fabry-Pérot cavity, ζ the antinodal factor corresponding to the QW's interface, l the QW's shape, L the cavity's thickness and d the distance between the QW and the metal mirror. Our normalization procedure cancels out ζ and L *at normal incidence*, but information about d is still contained in the large angle behavior.) Finally, we normalize the obtained FFP along θ by $\cos^2\theta$ to reveal the large-angle behavior [Figs. 3(b) and 3(e)]. We then apply the same procedure to the calculated FFP: flattening the Fabry–Pérot peaks to 1 at $\theta=0°$ and normalizing by $\cos^2\theta$.

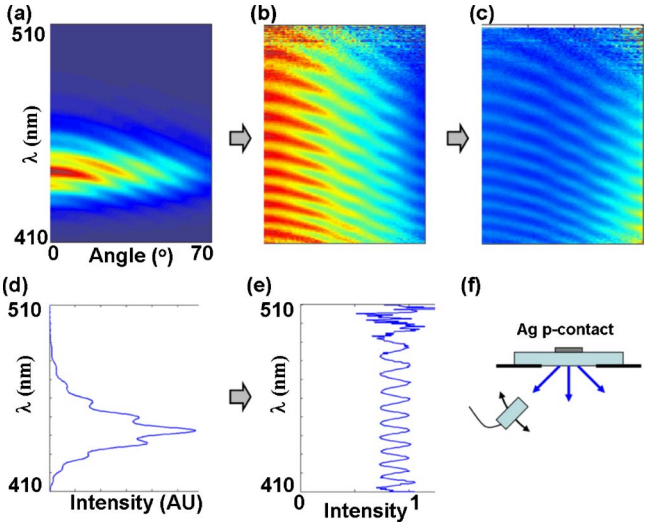

FIG. 3. (Color online) Normalization procedure of angle-resolved spectra. The raw spectrum (a) is normalized iteratively along the λ axis in order to flatten the Fabry–Pérot fringes (b), and then normalized by $\cos^2\theta$ along the θ axis in order to reveal the information at high angles (c). (d) and (e), respectively, show vertical cross sections of (a) and (b) at $\theta=0°$. (f) Geometry of the angular measurement.

Since the normalization along λ is arbitrary, we can no longer compare the data for different wavelengths (indeed, all information is lost along the $\theta=0°$ axis, where all the peaks are forced to 1). On the other hand, a known function is used along θ so that we can still compare, for a given λ, the values at $\theta=0°$ and at large θ. In practice, the information on the emitting QWs is thus contained in the large-angle region of the normalized FFP.

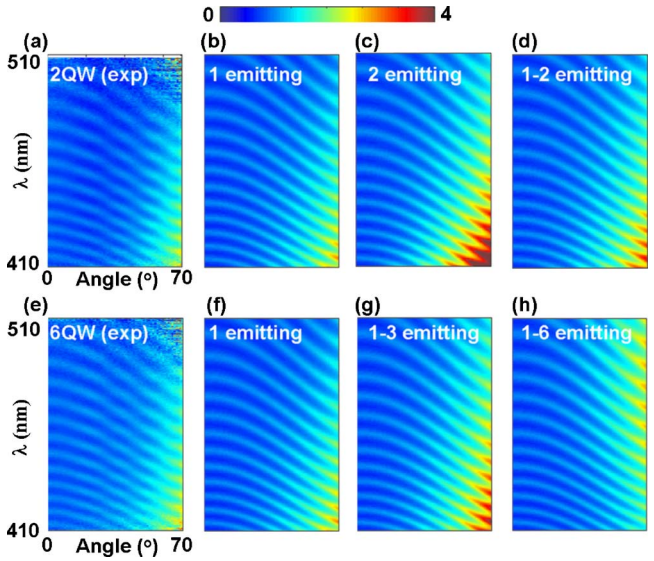

FIG. 4. (Color online) Normalized emission from a two QW and a six-QW structure. (a) Two-QW measurement. [(b)–(d)] Fits by QW 1, QW 1 and 2, and QW 2, respectively. (e) Six-QW measurement. [(f)–(h)] Fits by QW 1, QW 1–3, and QW 1–6, respectively. All plots use the same color scale, where the maxima of the Fabry–Pérot peaks at $\theta=0°$ are set to 1.

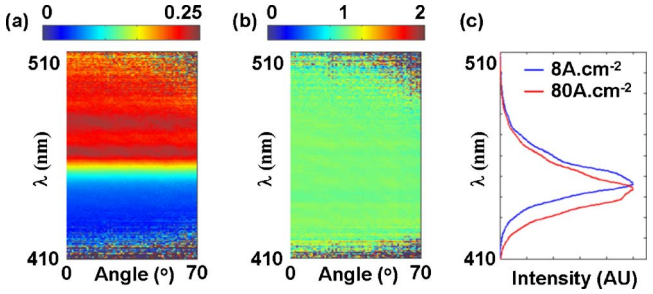

FIG. 5. (Color online) (a) Ratio R of angular measurements for the six-QW sample at current densities $J=8$ A cm^{-2} and $J=80$ A cm^{-2}. (b) Same as (a), normalized along λ to cancel out the blueshift of emission with J: the resulting ratio has no dependence along θ. (c) Approximate corresponding line shapes evidencing the blueshift with J.

Figure 4 shows the normalized experimental FFPs for the two QW and the six QW samples, together with several theoretical fits. First, let us note that the experimental FFPs are nearly identical for both samples. In itself, this is a strong indication that only the two first QWs (at most) emit light in the six-QW sample; emission from QWs 3–6 would strongly alter the FFP. For the two-QW sample, we consider fits by emission from QW 1 alone, QWs 1 and 2 (with equal intensity), and QW 2 alone. An excellent fit is obtained with QW 1 only emitting, while both other scenarios give poor fits, overestimating the signal at large θ and short λ. For the six-QW sample, we show fits by emission from QW 1 alone, QWs 1–3 (with equal intensity), and QWs 1–6 (with equal intensity). Again, the best fit is obtained for QW 1 only emitting. Many other fits corresponding to various QW populations were considered (not shown), and none yields a better match.

The above results correspond to high current operation. To check for lower-current behavior and possible evolution of the QW population with J, we collected additional FFPs on the same samples at lower J (8.0 and 0.8 A cm^{-2}). Figure 5 displays the ratio R of the FFP at $J=8$ A cm^{-2} by the FFP at $J=80$ A cm^{-2}. Again, any difference in the carrier distribution in QWs between low and high J should result in a different angular distribution. However, Fig. 5(a) shows no angular dependence: the only remarkable feature is a drop in R at short wavelengths, but without any angular component. This indicates that the same QW population occurs at both currents (namely, only QW 1 emits). The drop of R at short λ simply manifests the blueshift in the QW emission at high J [Fig. 5(c)]. The analysis is made more obvious on Fig. 5(b), where we normalize R along λ as previously in order to cancel this shift (i.e., by normalizing the data to 1 along $\theta=0°$). (No angular normalization is necessary in this case, since taking the ratio of the two spectra naturally removes angular effects.) The normalized ratio is then constant over the full λ-θ plane, excluding any variation in the QW population. A similar observation holds at even lower current $J=0.8$ A cm^{-2}.

Finally, let us point out that similar experiments were repeated on other samples with similar growth parameters, but using various p-layer thicknesses in order to optically probe the QWs in a different way (specifically, the p-layer thickness was tuned to minimize light extraction from QWs 1 and 2, making the measurements more sensitive to potential light emission from other QWs). In all cases, the results are consistent with emission from the p-side QW alone, and never suggest that more than 20% of the emission may come from the next QW.

In conclusion, we have studied conventional (0001) InGaN LEDs with varying number of QWs to explore the possibility of decreasing the carrier density in each well. No matter how many QWs are grown, spontaneous emission only occurs in the p-side QW. This suggests that high-power devices require specific efforts in order to push the peak efficiency to higher current. One approach is to modify the design of the QW active region to improve carrier spreading. Another approach was also reported recently in Ref. 3, where the QWs are replaced by a double heterostructure, ensuring uniform carrier spreading across the active region and a lower carrier density.

[1] M. R. Krames, O. B. Shchekin, R. Mueller-Mach, G. O. Mueller, L. Zhou, G. Harbers, and M. G. Craford, J. Disp. Technol. **3**, 160 (2007).
[2] T. Mukai, M. Yamada, and S. Nakamura, Jpn. J. Appl. Phys., Part 1 **38**, 3976 (1999).
[3] N. F. Gardner, G. O. Mueller, Y. C. Shen, G. Chen, S. Watanabe, W. Gotz, and M. R. Krames, Appl. Phys. Lett. **91**, 243506 (2007).
[4] Y.-C. Shen, G. O. Mueller, S. Watanabe, N. F. Gardner, A. Munkholm, and M. R. Krames, Appl. Phys. Lett. **91**, 141101 (2007).
[5] H. Benisty, H. De Neve, and C. Weisbuch, IEEE J. Quantum Electron. **34**, 1612 (1998).
[6] Y. C. Shen, J. J. Wierer, M. R. Krames, M. J. Ludowise, M. S. Misra, F. Ahmed, A. Y. Kim, G. O. Mueller, J. C. Bhat, S. A. Stockman, and P. S. Martin, Appl. Phys. Lett. **82**, 2221 (2003).
[7] H. Benisty, R. Stanley, and M. Mayer, J. Opt. Soc. Am. A **15**, 1192 (1998); We assume an in-plane dipole distribution, corresponding to heavy hole-electron transitions. This is supported both by theoretical band structure arguments (Refs. 9 and 10) and by experimental measurements (Ref. 11). The small wiggles in the curves of Fig. 2(b) are caused by guided modes being cut off in the GaN layer.
[8] P. M. Pattison, A. David, R. Sharma, C. Weisbuch, S. P. DenBaars, and S. Nakamura, Appl. Phys. Lett. **90**, 031111 (2007).
[9] S. L. Chuang and C. S. Chang, Phys. Rev. B **54**, 2491 (1996).
[10] I. Vurgaftman and J. R. Meyer, J. Appl. Phys. **94**, 3675 (2003).
[11] M. F. Schubert, S. Chhajed, J. K. Kim, E. F. Schubert, and J. Cho, Appl. Phys. Lett. **91**, 051117 (2007).